



Sharif University of Technology

Scientia Iranica

Transactions A: Civil Engineering

www.scientiairanica.com



Investigating climate change impact on extreme rainfall events

Case study: Chenar-Rahdar basin, Fars, Iran

A. Pourtouserkani* and Gh. Rakhshandehroo

Department of Civil and Environmental Engineering, School of Engineering, Shiraz University, Zand Blvd., Shiraz, 7134851156, Iran.

Received 21 January 2013; received in revised form 28 September 2013; accepted 19 October 2013

KEYWORDS

Climate change;
Extreme events;
Downscaling;
Change factor;
LARS-WG;
SDSM.

Abstract. In this research, the impact of climate change on extreme rainfall events in the Chenar-Rahdar Basin, Shiraz, Iran, was investigated utilizing three statistical downscaling methods, namely, change factor, LARS-WG, and SDSM. Daily precipitations with different recurrence periods were projected for the future period of 2011-2040 (2020s), based on two AOGCM output data (HadCM3 and CGCM3), under an A2 emission scenario. In summary, HadCM3 (for three downscaling methods) projected an increasing trend (of up to 21.8%) in extreme rainfall events for the period of 2011-2040, with respect to the base period. On the other hand, CGCM3 showed an increasing trend for extreme rainfall events for the first two methods (up to 24.7%), while the SDSM method resulted in an increasing trend (up to 3.6%) for recurrence periods of 20 and 25 years and a very small decreasing trend (down to -2%) for recurring periods of 50 and 100 years. Relatively low correlation coefficients in multiple regressions obtained for both AOGCMs reflect the limitations of SDSM in downscaling precipitation data in the study area. Comparing the three downscaling techniques utilized in this study, it is concluded that using change factor or LARS-WG downscaling methods would be conservative enough in climate change impact assessment for the next 30 years.

© 2014 Sharif University of Technology. All rights reserved.

1. Introduction

A change in climate leads to changes in the frequency, intensity, spatial extent, duration, and timing of extreme weather and climate events, and can result in unprecedented extreme weather and climate events [1]. In particular, climate models suggest an increase in rainfall intensities in the northern hemisphere under enhanced greenhouse conditions [2]. As a result,

researchers anticipate that the frequency of heavy precipitation or proportion of total rainfall from heavy falls will increase in the 21st century over many areas of the globe. This is particularly the case in high latitudes and tropical regions and in winters in the northern mid-latitude [1-5].

Atmospheric-Oceanic General Circulation Models (AOGCMs) are usually used to project changes in atmospheric variables under the climate change scenarios defined by the Intergovernmental Panel for Climate Change (IPCC) [6]. Output data from AOGCMs are typically coarse-gridded with 150~300 km grid spacing and may be projected for each cell with ~50000 km² area. However, a much finer resolution is needed for climate change impact assessments, and, hence,

*. Corresponding author. Tel.: 0098 9171181650;
Fax: 0098 7116473161
E-mail addresses: amirpot@yahoo.com (A. Pourtouserkani); rakhshan@shirazu.ac.ir (Gh. Rakhshandehroo)

downscaling techniques are often used to transform coarse-gridded data from AOGCMs to fine-gridded ones. Fine-gridded data are usually extracted by Regional Climate Models (RCMs) for cells of 12~50 km grid spacing.

Two main downscaling techniques most often used in climate change impact assessment research are dynamical and statistical downscaling methods [7]. Dynamical downscaling involves the nesting of a higher resolution RCM within a coarser resolution General Circulation Model (GCM). Statistical downscaling methods, on the other hand, involve establishing a statistical relationship between large scale climatic conditions, and local variety based on historical data. Statistical downscaling techniques are easier and less costly in comparison with dynamical techniques, and are the most used in anticipated hydrologic impact studies under climate change scenarios [8]. Some statistical downscaling methods used in climate change impact assessments are the Statistical Down Scaling Model (SDSM), the stochastic weather generator (LARS-WG), the change factor, and weather typing.

Several researchers have been working on climate change impact worldwide using different downscaling techniques and comparing the results. They have shown that different downscaling techniques may yield different results; a fact that is usually attributed to uncertainties in the techniques, climate change scenarios, GCM outputs, and differences in the structure of the techniques [9-12].

Yimer et al. (2009) investigated climate change hydrological response of the Beles river basin, as the upper Blue Nile, in Ethiopia. They used the SDSM method for downscaling temperature and precipitation data based on the A2a emission scenario and the HadCM3 atmospheric model for 2050. They applied a rainfall-runoff model to transform downscaled rainfall data to runoff and to predict future Beles river flow. Their studies showed a projected decrease in annual runoff; most of it being in the summer season, the main rainy season of the area [13].

Segui et al. (2010) studied climate change impact on French Mediterranean basins. They used output data of an atmospheric-oceanic regional climate model and utilized three downscaling techniques; a statistical method based on weather regime, a quantile-mapping method, and the method of anomaly (change factor). They used 1970-2000 (end of 20th century) as the base period, and 2035-2065 (middle of the 21st century) as the future period. The three downscaling techniques showed the same changes in mean annual precipitation in temporal scale, while the spatial rainfall patterns of the three methods were completely different. They concluded that statistical downscaling based on weather typing is not a suitable method for generating extreme events. Moreover, most of the stations in their study

area showed decreasing trends in river flow, especially during the summer [14].

Sunyer et al. (2012) studied climate impact on extreme rainfall in northern Copenhagen, Denmark. They compared five statistical downscaling methods, based on a common change factor methodology, using results from four different RCMs driven by different GCMs. The downscaling methods were mean change factor, mean and variance change factor, Markov chain weather generator, LARS-WG, and Neyman-Scott rectangular pulse weather generator. They generated time series for 2071-2100 based on the A1B emission scenario. Results showed an increase in extreme rainfall events for three out of four RCMs. The major uncertainties of this study were related to the variability of RCM output and downscaling methods [6].

Dibike and Coulibaly (2005) studied hydrological climate change impact assessment on the Saguenay watershed in northern Quebec, Canada. They applied two statistical downscaling techniques: SDSM regression based and the LARS-WG stochastic weather generator, and generated future temperature and precipitation based on CGCM1 output data and an A2 emission scenario. They showed that the daily precipitation trend and its variability, based on the SDSM downscaling technique, is increasing for future periods of 2020s, 2050s, and 2080s, while there is no obvious trend for the time series downscaled with LARS-WG. They attributed the difference to SDSM usage of any relevant large-scale climate (predictor) variable from GCM outputs as input to estimate the corresponding local-scale predictant such as precipitation, while LARS-WG used the relative change in the GCM outputs of only those variables which directly correspond to those predicted; hence, producing different results [12].

Massahbavani and Sadatashofteh (2011) studied climate change impact on the Aidoghmosh basin, East Azerbaijan, Iran, for the 2040-2069 period, based on the A2 emission scenario and HadCM3 atmospheric model. They downscaled monthly temperature and precipitation data, using proportional downscaling as a spatial and change factor, as a temporal downscaling technique. Their results showed 30~40 percent change in precipitation in the future, with respect to the base period (1971-2000) [15].

Goodarzi et al. (2011) studied climate change impact in the Azamharat river basin, in an arid region of Yazd, Iran. They used CGCM3 output data based on the A2 emission scenario, and applied proportional and change factor downscaling techniques as spatial and temporal downscaling, respectively. Their results for the period of 2010-2039 with the base period of 1982-2008 showed an increase in precipitation in December, January, February, and April and a decrease in other months of the year [16]. To the best of the authors'



Figure 1. Chenar-Rahdar basin: (a) Satellite view; and (b) GIS basin modeled view.

knowledge, climate change impact on extreme rainfall events in Iran has not been studied utilizing different downscaling techniques. In this research, climate change impact on extreme precipitation is investigated using two AOGCM model outputs (HadCM3 and CGCM3). Atmospheric model precipitation output data were downscaled (from monthly to daily) for the future period of 2020s (2011–2040) using three statistical downscaling techniques. Change factor, LARS-WG stochastic weather generator, and SDSM, along with a proportional downscaling method, were used at the Chenar-Rahdar basin, Fars, Iran. Based on the precipitation time series generated by downscaling techniques, maximum 24-hour precipitations for the two AOGCM models were extracted and a frequency analysis was performed to get future daily precipitations with different recurrence periods.

2. Study area

The Chenar-Rahdar river basin, studied in this research, lays south east of Shiraz, Iran, between $29^{\circ}, 33'$ to $29^{\circ}, 44'$ northern latitude and $52^{\circ}, 15'$ to $52^{\circ}, 26'$ eastern longitude. Its elevation ranges from 1619 m to 2870 m, with average elevation of 2033 m above mean sea level. The area of the basin up to the Chenar-Rahdar hydrometric station (at $29^{\circ}, 37', 03''$ N, $52^{\circ}, 25', 29''$ E with elevation of 1637 m above mean sea level) is 174 km². The Chenar-Rahdar river originates from Shiraz eastern highlands of Paskoohak, Garoo,

Sorkh, and Pirbord mountains and ends in Maharloo Lake, ~ 30 km downstream of the hydrometric station (Figure 1).

Low river capacity, along with a very mild river slope downstream of the station, adds to the vulnerability of these areas, with respect to low amounts of flow increase. In fact, these regions are known as damage centers, and climate change impact assessment in the basin plays an essential role in area vulnerability evaluation.

For climate change impact assessment, 30 years of recorded precipitation data (1971–2000) at the Chenar-Rahdar rain gage station, located at the basin outlet (Figure 1), were used as the base period data. Output data from two atmospheric models (HadCM3 and CGCM3) were extracted for 2011–2040 at the Chenar-Rahdar station. The A2 emission scenario (IPCC 4th report) was considered and hydro meteorological data were exploited from the Canadian Climate Change Scenario Network (www.cccsn.ca) [17].

3. Climate change simulation methods

Three downscaling methods (change factor, stochastic weather LARS-WG, and regression based SDSM) were used to simulate climate change and scenario generation for 2020s, based on spatial proportional downscaling at average elevation of the basin for the base period. Precipitation time series were generated and extreme rainfall magnitudes were estimated by

methods using frequency analysis, and the results were compared.

3.1. Change factor

In this method, average monthly precipitation changes for a future period were extracted from the two AOGCMs based on the A2 emission scenario. Precipitation change factor, Δp , calculated by Eq. (1) was used as the base of the calculation for climate change impact assessment:

$$\Delta P_i = \overline{P}_{\text{GCM,FUT},i} / \overline{P}_{\text{GCM,base},i}, \quad (1)$$

$\overline{P}_{\text{GCM,FUT},i}$ Simulated 30-year average precipitation for a future period from AOGCM for month i ;

$\overline{P}_{\text{GCM,base},i}$ Simulated 30-year average precipitation for the base period from AOGCM for month i .

Precipitation time series for a future period were down-scaled using Eq. (2). Then, maximum 24-hour (daily) precipitations for both models (HadCM3 and CGCM3) were extracted and frequency analysis was performed to get precipitations with different recurrence periods:

$$P_{\text{FUT},i} = P_{\text{OBS},i} * \Delta P_i, \quad (2)$$

$P_{\text{FUT},i}$ Downscaled future precipitation time series for month i ;

$P_{\text{OBS},i}$ Observed precipitation time series for month i based on the rainfall gauge data.

3.2. Stochastic weather generator LARS-WG

The LARS-WG (Long Ashton Research Station) is stochastic weather generator software that has the capability of modeling weather in a site based on observed data, and using the model to extend data for the future. These data are usually climatological variable time series, such as minimum and maximum temperature, precipitation, and solar radiation [18].

LARS-WG operates based on the series weather generator described in Racsco et al. [19]. This model utilizes Semi-Empirical Distributions (SEDs) for lengths of wet and dry day series, daily precipitation, minimum and maximum temperature, and daily solar radiation.

The distribution, $\text{Emp} = \{a_o, a_i, h_i, i = 1, 2, \dots, 23\}$, is a histogram with 23 intervals, $[a_{i-1}, a_i]$, where $a_{i-1} < a_i$ and h_i denote the number of events observed in the i th interval. Random values from the SED are chosen by first selecting one of the intervals, using a proportion of events in each interval as selection probability, and then selecting a value within that interval from a uniform distribution.

Such a distribution is flexible, and can approximate a wide variety of shapes by adjusting the intervals, $[a_{i-1}, a_i]$ [18,19].

The SED used in LARS-WG requires 24 parameters for boundary values and 23 parameters as the number of events in each interval. Simulation of precipitation occurrence is modeled by alternating wet and dry series (days), where a wet day is defined as a day with precipitation greater than zero. The length of each series is chosen randomly from the wet or dry SED for the month in which the series starts. In determining the distributions, observed series are also allocated to the month in which they start. For a wet day, the precipitation value is generated from the SED for the particular month, independent of the length of wet series or the amount of precipitation on previous days [18]. LARS-WG has the ability to consider climate change using a climate change scenario for future data generation based on monthly AOGCM output data or a scenario file manually inserted into the program [18].

In order to generate a future precipitation time series by the model, daily precipitation at the basin for the base period of 1971-2000 was introduced to the model, and its statistical distribution was found via calibration and tested via validation. Statistical tests were utilized for goodness-of-fit analysis during the calibration stage. For validation, on the other hand, synthetic data for the base period were generated and compared with observed data. Once calibration and validation were over, future precipitation time series were generated using the best fitted distribution. Then, maximum 24-hour (daily) precipitations for HadCM3 and CGCM3 were extracted, and frequency analysis was performed to get precipitations with different recurrence periods.

3.3. SDSM linear regression model

SDSM, developed in England (2002), utilizes a combination of regression methods (transfer functions) and synthetic weather generation for downscaling. In this model, local climatic characteristics are expressed as regional large scale climatic conditions in the form of $R = F(X)$, in which R is a downscaled climatic variable and F is the transfer function to be obtained based on historical data analysis. Prediction of future climatic variables influenced by the climate change phenomenon is accomplished by establishing statistical relations between large scale predictor variables and small scale predictand variables [7].

To calibrate the SDSM, daily observed large scale variables at base period, 1971-2000, were extracted from NCEP as independent variables and entered into the model, in company with daily observed precipitation at the basin during the same period, as a dependent variable. In order to evaluate the ability

of AOGCMs in modeling precipitations, large scale variables (predictors) simulated by two AOGCMs (i.e. HadCM3, CGCM3) for the base period were entered to the calibrated SDSM. Downscaled precipitation was generated and compared with the observed data. Finally, daily precipitation time series were generated by the calibrated SDSM, based on future period large scale variables of both AOGCMs (i.e. HadCM3, CGCM3). Predictor variables for the study area are available on the Canadian Climate Change Scenario Network web site (www.cccsn.ca) for both AOGCM models.

Maximum daily precipitations that are extracted from daily precipitation time series given by the spatial downscaling of GCM outputs using SDSM methods, are often not comparable to observed maximum daily precipitations at a local site. Therefore, an adjustment procedure (bias correction) is needed to improve the accuracy of the spatial downscaling SDSM technique in the estimation of local maximum daily precipitations [20].

4. Results and discussions

4.1. Change factor downscaling technique

Frequency analysis was performed for maximum 24-hr precipitations extracted from the base period time series, along with the future downscaled time series, using a change factor downscaling technique. Results showed that for the base period, 2 parameter Gamma distributions, and, for the future period, Log Pearson type III for HadCM3 and Gumbel distribution for CGCM3, were the best frequency distributions fitted to the data. Figure 2 shows precipitation with different recurrence periods based on the change factor method and two AOGCMs for the future period.

As shown in Figure 2, the daily precipitation probability trend for HadCM3 deviated upward compared to the base period, especially for less frequent events. In particular, daily precipitation for 20, 25, 50 and 100-year recurrence periods (extreme events) increased by 14.2, 15.3, 18.5 and 21.8 percent, respectively, in comparison with the base period. On the

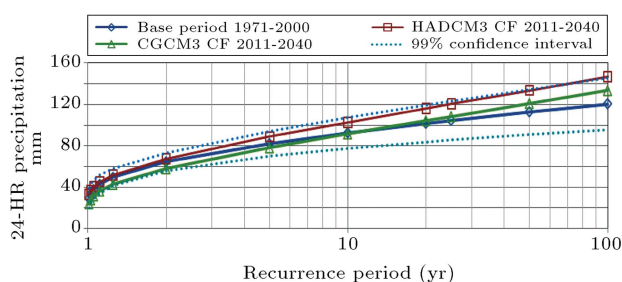


Figure 2. Maximum daily precipitations with different recurrence periods analyzed by change factor downscaling technique, based on two AOGCMs for the future period (2011-2040).

other hand, for the CGCM3 model, such a precipitation trend is somewhat different. Daily future precipitations decreased for 10-year and smaller recurrence periods, and increased for longer recurrence periods. In particular, 20, 25, 50, and 100 year recurrence periods (extreme events) increased by 2.7, 3.9, 7.4 and 10.9 percent, respectively, in comparison with the base period, which is a lower increase compared to the HadCM3 model. As shown, for both AOGCMs, the daily future precipitation trend lies within a 99% confidence interval of the base period.

4.2. LARS-WG stochastic weather generator downscaling technique

Statistical tests were used to calibrate the model and, then, synthetic time series were generated for the base period and compared with observed data. Maximum daily precipitations extracted from the time series generated at the base period showed standard deviation of 12.9 mm, while this statistic for the observed values was 19.1 mm. Comparison between maximum daily precipitations generated by the LARS model and observed values resulted in $PRMSE = 30.3$ mm and $MAE = 25$ mm.

Figure 3 shows observed and LARS-generated values for maximum daily precipitations with different recurrence periods at the base period. Comparison of the results for 2, 5, 10, 20, 25, 50 and 100 year recurrence periods showed acceptable indices of $RMSE = 21$ mm, $MAE = 20.8$ mm, and $R^2 = 0.99$. Relatively low RMSE and MAE, in addition to a high correlation coefficient, verify the high performance of the model for data generation.

Future precipitation time series were generated by the verified model, based on scenario files introduced to the model. Maximum daily precipitations for the future period of 2011-2040 (2020s) were extracted from the generated time series and frequency analysis was performed. 2-parameter Gamma distribution for HadCM3 and 3-parameter Log-normal distribution for CGCM3 were the best frequency distributions for daily

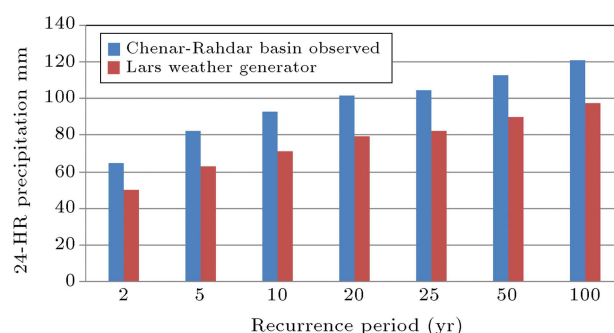


Figure 3. Comparison between observed and LARS-WG generated maximum daily precipitation with different recurrence periods for the base period; $RMSE = 21$ mm, $MAE = 20.8$ mm.

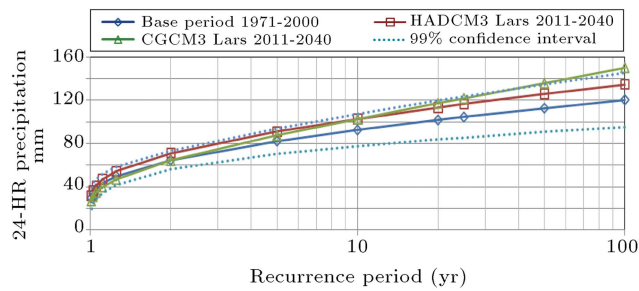


Figure 4. Precipitation with different recurrence periods analyzed by LARS-WG downscaling technique based on two AOGCMs data for the future period (2011-2040).

precipitations. Figure 4 shows daily precipitation with different recurrence periods, by LARS-WG, for the base and future periods, under climate change impact for the two AOGCMs.

As shown in Figure 4, for both AOGCMs (HadCM3 and CGCM3), the daily precipitation probability trend deviates upwards compared to the base period, especially for less frequent events. In particular, in the case of HadCM3, daily precipitation for 20, 25, 50 and 100 year recurrence periods (extreme events) increased by 11.2, 11.3, 11.5 and 11.7 percent, respectively, in comparison with the base period. On the other hand, for the CGCM3 model, this increase was 15.3, 16.6, 20.7, and 24.7 percent for 20, 25, 50, and 100 year recurrence periods as extreme events, respectively (Figure 4). This behavior is similar to the results for the HadCM3 model using a change factor downscaling technique. As shown, the future daily precipitation trend for both AOGCMs lies within a 99% confidence interval near the upper band, except for the CGCM3 model, where the daily precipitation trend lies outside the 99% confidence interval for recurrence periods longer than 50 years.

4.3. SDSM downscaling technique

First, a screening of downscaling predictor variables was followed to select large-scale variables (predictors) which correlate to the small-scale one (predictand). Many predictors were investigated, seeking the ones with highest correlation. The search was performed utilizing scatter plots and partial correlation analysis.

In the calibration process, a downscaling model was constructed based on multiple regression equations, and parameters for the regression between predictors and predictand were found. Variables listed in Tables 1 and 2 demonstrated the highest correlation coefficients between predictors and predictand, with $R^2 = 0.243$ and $R^2 = 0.189$ for HadCM3 and CGCM3, respectively. Relatively low correlation coefficients for the two AOGCMs reflect the limitations of the SDSM model in downscaling precipitation data.

A weather generation operation in SDSM was used to construct ensembles of synthetic daily pre-

Table 1. Predictor variables from NCEP in HadCM3 databank used for SDSM calibration and weather generation.

No	Predictors	Description
1	p-zaf	Surface vorticity
3	p500 af	500 hpa geo-potential height
4	r500 af	Relative humidity at 500 hpa
5	r850 af	Relative humidity at 850 hpa

Table 2. Predictor variables from NCEP in CGCM3 databank used for SDSM calibration and weather generation.

No	Predictors	Description
1	p-zgl	Surface vorticity
2	p-zhgl	Surface divergence
3	p5-ugl	500 hpa zonal velocity
4	p500gl	500 hpa geo-potential height
5	s500gl	Specific humidity at 500 hpa
6	shumgl	Surface specific humidity
7	tempgl	Mean temperature at 2m

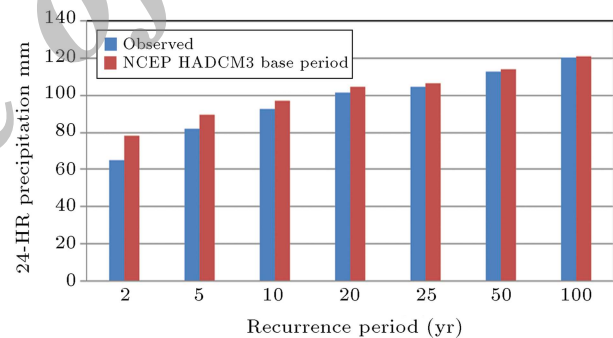


Figure 5. Maximum daily precipitation with different recurrence period simulated by SDSM model based on NCEP data at the base period versus observed data; RMSE = 6.2 mm, MAE = 4.6 mm, $R^2 = 0.99$.

cipitation series, given observed atmospheric predictor variables and regression model weights produced by calibration. Bias correction was used for any tendency in the downscaling model to over or under-inflate the variance of the conditional process [21]. Furthermore, bias correction values were tested in the SDSM model to adjust simulated maximum daily precipitation values with different recurrence periods to obtain minimum errors, with respect to observed values at the base period. Through this adjustment, standard deviation of maximum daily precipitation, based on downscaled data for NCEP values from the HADCM3 and CGCM3 data bank, increased from 8.1 mm and 6.7 mm to 13.1 mm and 13 mm, respectively. Figures 5 and 6 show comparisons between maximum daily precipitation, with 2, 5, 10, 20, 25, 50 and 100 year recurrence

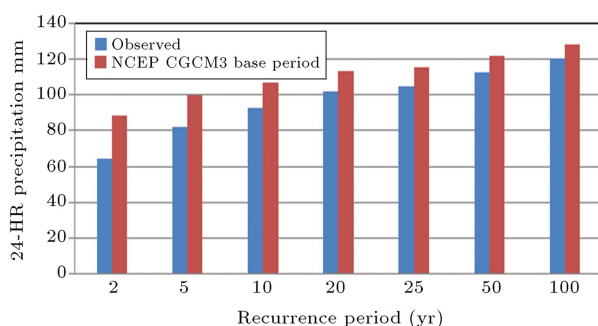


Figure 6. Maximum daily precipitation with different recurrence period downscaled by SDSM model based on NCEP CGCM3 data at the base period versus observed data; RMSE = 14.2 mm, MAE = 13.3 mm, $R^2=0.99$.

periods generated by SDSM (based on NCEP data in HadCM3 and CGCM3 databanks) for the base period and the observed data at the basin. As shown in Figure 5, comparison between NCEP HadCM3 and observed data for different recurrence periods resulted in RMSE = 6.2 mm, MAE = 4.6 mm and a correlation coefficient of $R^2 = 0.99$. Comparison between NCEP CGCM3 data and observed precipitation, however, resulted in RMSE = 14.2 mm, MAE = 13.3 mm and a correlation coefficient of $R^2 = 0.99$ (Figure 6). Relatively high correlation coefficients and low errors in both models reflect the suitable selection of predictor variables.

Once models were calibrated and verified, output data from two AOGCMs (HadCM3 and CGCM3) were downscaled and compared with observed data at the base period. In the course of downscaling HadCM3 and CGCM3 data, the bias correction procedure showed increases in the standard deviation of maximum daily precipitations from 6.4 mm and 10.7 mm to 14.4 mm and 14.1 mm at the base period, respectively. Apparently, the bias correction adjusted standard deviations to values closer to the standard deviation of observed maximum daily precipitations at the base period (i.e. 19.1 mm).

Figures 7 and 8 depict evaluation results for several bias correction trials in the SDSM model for HadCM3 and CGCM3, respectively. As shown, comparison between observed and generated values for different recurrence periods reflects RMSE = 5.1 mm, MAE = 4.1 mm, $R^2 = 0.99$ for HadCM3 (Figure 7), and RMSE = 10 mm, MAE = 9.2 mm, $R^2 = 0.99$ for CGCM3 (Figure 8).

Considering the fewer errors in HadCM3, one may conclude that this model would simulate climate change phenomenon better than CGCM3 for future periods. However, both models were utilized for scenario generation in the future.

The calibrated file at the base period was utilized by SDSM to generate a precipitation time series for both AOGCMs. Maximum daily precipitations for

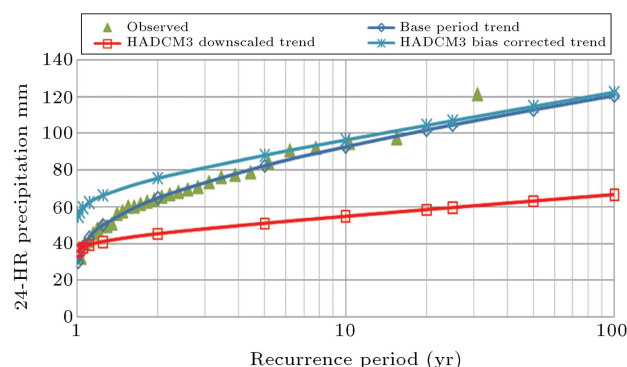


Figure 7. Evaluation of HADCM3 model by SDSM for maximum daily precipitation with different recurrence periods after bias correction at the base period; RMSE = 5.1 mm, MAE = 4.1, $R^2=0.99$.

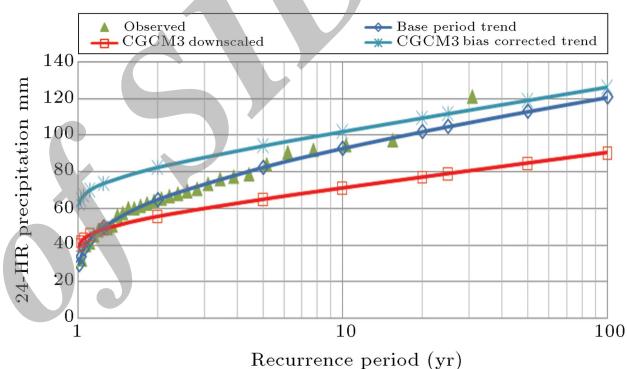


Figure 8. Evaluation of CGCM3 model by SDSM for maximum daily precipitation with different recurrence periods after bias correction at the base period; RMSE = 10 mm, MAE=9.2 mm, $R^2 = 0.99$.

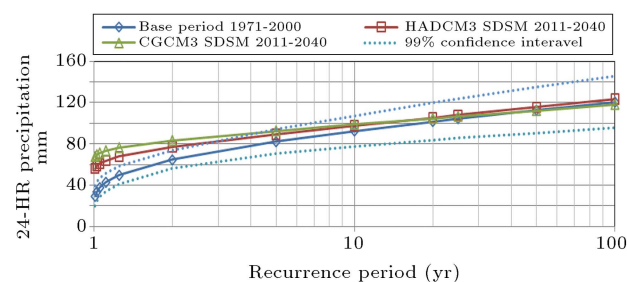


Figure 9. Precipitation with different recurrence periods analyzed by SDSM downscaling technique, based on the two AOGCMs for the future period (2011-2040).

the future period, 2011-2040 (2020s), were extracted from the generated series, and frequency analysis was performed to obtain daily precipitations with different recurrence periods (Figure 9). Gumbel distribution for both HadCM3 and CGCM3 was the best frequency distribution fitted to the data.

Figure 9 indicates that, in the case of HadCM3, daily precipitations for 20, 25, 50 and 100 year recurrence periods (extreme rainfalls) increase by 3.6, 3.2, 2.5 and 2.2 percent, respectively, with respect to the

base period. In the case of CGCM3, daily precipitations for 20 and 25 year recurrence periods increase 2.9 and 1.9 percent, respectively. For 50 and 100 year recurrence periods, however, slight decreases of 0.4 and 2 percent, with respect to the base period, were observed. As shown in Figure 9, the daily precipitation distribution trend lies within a 99% confidence interval for recurrence periods longer than 5 years for both HadCM3 and CGCM3 models. On the whole, one may conclude that the daily precipitation distribution trend slightly differs from the observed trend at the base period, indicating a small climate change impact on extreme rainfall for the 2011-2040 period.

5. Conclusions

The impact of climate change on extreme rainfall events in the Chenar-Rahdar basin, Fars, Iran, was investigated utilizing three statistical downscaling methods, namely, change factor, LARS-WG, and SDSM. Daily precipitations with different recurrence periods were projected for the future period of 2011-2040 (2020s) based on two AOGCM output data (HadCM3 and CGCM3) under the A2 emission scenario. According to HadCM3, future daily precipitations increased up to 21.8% compared to the base period when using the change factor downscaling technique. For CGCM3, on the other hand, daily future precipitations slightly decreased for small recurrence periods ($t \leq 10$ yr), and increased (up to 10.9%) for longer periods ($t > 10$ yr). It may be concluded that for both AOGCMs, the occurrence probability of extreme events in the future increases, however, less for CGCM3 compared to HadCM3. The LARS-WG technique projected increases in future daily precipitations for both AOGCMs. The increases were up to 11.7% and 24.7% compared to the base period for HadCM3 and CGCM3, respectively. Furthermore, the occurrence probability of extreme events showed a much higher increase in CGCM3 compared to HadCM3. The SDSM technique projected small changes in future daily precipitation for both AOGCMs. Similar to other methods, in the case of HadCM3, extreme rainfall increased up to 3.6 percent compared to the base period. For the case of CGCM3, no significant change was seen. Furthermore, similar to the first two methods for HadCM3, the occurrence probability of extreme rainfall events increased, while, for CGCM3, remained almost unchanged.

In summary, HadCM3 (for three downscaling methods) projected an increasing trend (of up to 21.8%) in extreme rainfall events for the 2011-2040 period, with respect to the base period. On the other hand, CGCM3 showed an increasing trend for extreme rainfall events for the first two methods (up to 24.7%), while the SDSM method resulted in an

increasing trend (up to 3.6%) for recurrence periods of 20 and 25 years and a very small decreasing trend (down to -2%) for recurrence periods of 50 and 100 years. The fact that SDSM utilizes large-scale climate variables from HadCM3 and CGCM3 outputs as input to estimate local-scale precipitation, apparently, makes its output less reliable compared to LARS-WG and the change factor, which use AOGCM output variables directly corresponding to precipitation. Relatively low correlation coefficients in multiple regressions obtained for both AOGCMs also reflect the limitations of SDSM in downscaling precipitation data in the study area. It is concluded that using the change factor or LARS-WG downscaling methods would be conservative enough in climate change impact assessment for the next 30 years.

Acknowledgment

Authors would like to thank and acknowledge the assistance and effort supplied by the Water Organization of Fars Province for providing the source data.

Nomenclature

AOGCM	Atmospheric Oceanic General Circulation Model
LARS-WG	Long Ashton Research Station-Weather Generator
SDSM	Statistical Down Scaling Model
HadCM3	Hadley Centre Coupled Model, version3
CGCM3	Coupled Global Climate Model, third generation
CF	Change Factor
IPCC	Intergovernmental Panel for Climate Change
GCM	General Circulation Model
RCMs	Regional Climate Models
SED	Semi-Empirical Distribution
RMSE	Root Mean Squared Error
MAE	Mean Absolute Error
NCEP	National Centers for Environmental Prediction
R	Correlation Coefficient

References

- Curry, J. "IPCC special reports on extreme events", *Intergovernmental Panel on Climate Change (IPCC)* (2011).
- Ekstrom, M., Fowler, H.J., Kilsby, C.G. and Jones, P.D. "New estimates of future changes in extreme rainfall across the UK using regional climate model integrations. 2. Future estimates and use in impact

- studies". *Journal of Hydrology*, **300**, pp. 234-251 (2005).
3. Jones, P.D., Reid, P.A. "Assessing future changes in extreme precipitation over Britain using regional climate model integrations" *International Journal of Climatology*, **21**, pp. 1337-1356 (2001).
 4. McGuffie, K., Henderson-Sellers, A., Holbrook, N., Kothavala, Z., Balachova, O. and Hoekstra, J. "Assessing simulations of daily temperature and precipitation variability with global climate models for present and enhanced greenhouse climates", *International Journal of Climatology*, **19**, pp. 1-26 (1999).
 5. Palmer, T.N., Räisänen, J. "Quantifying the risk of extreme seasonal precipitation events in a changing climate", *Journal of Nature*, **415**, pp. 512-514 (2002).
 6. Sunyer, M.A., Madsen, H. and Ang, P.H. "A comparison of different regional climate models and statistical downscaling methods for extreme rainfall estimation under climate change", *Journal of Atmospheric Research*, **103**, pp. 119-128 (2012).
 7. Wilby, R.L. and Dawson, C.W. "A decision support tool for the assessment of regional climate change impact SDSM User Manual version 4.2", UK (2007).
 8. Sajjadkhan, M., Coulibaly, P. and Dibike, Y.B. "Uncertainty analysis of statistical downscaling methods" *Journal of Hydrology*, **319**, pp. 357-382 (2006).
 9. Samadi, S.Z. and Massahbavani, A. "Application of artificial neural network & statistical downscaling for prediction of future precipitation & temperature changes", *3th Conference Iran Water Resources Management*, October 14-16, Civil Engineering Department, Tabriz, Iran (In Persian) (2008).
 10. Fiseha, B.M., Melesse, A.M., Romano, E., Volpi, E. and Fiori, A. "Statistical downscaling of precipitation and temperature for the upper Tiber basin in central Italy", *International Journal of Water Sciences*, **1**, pp. 1-14 (2012).
 11. Chen, H., Xu, C.Y. and Guo, S. "Comparison and evaluation of multiple GCMs statistical downscaling and hydrological models in the study of climate change impacts on runoff", *Journal of Hydrology*, **434-435**, pp. 36-45 (2012).
 12. Dibike, Y.B. and Coulibaly, P. "Hydrologic impact of climate change in the Saguenay watershed", *Journal of Hydrology*, **307**, pp. 145-163 (2005).
 13. Yimer, G., Jonoski, A. and Griensven, V. "Hydrological response of a catchment to climate change in the upper Beles river basin, upper Blue Nile, Ethiopia", *Water Engineering Scientific Magazine*, **2**, pp. 49-59 (2009).
 14. Quintana Segui, P., Ribes, A., Martin, E., Habets, F. and Boe, J. "Comparison of three downscaling methods in simulating the impact of climate change on the hydrology of Mediterranean basins", *Journal of Hydrology*, **383**, pp. 111-124 (2010).
 15. Massahbavani, A. and Sadatashofteh, P. "Effect of climate change on maximum discharges: Case study: Aidoghmoosh watershed, East Azerbaijan, Iran" *Iranian Journal of Agricultural Science and Technology and Natural Resources*, **53**, pp. 25-39 (2010).
 16. Goodarzi, E., Massahbavani, A., Dastoorati, M. and Talebi, A. "Impact assessment of climate change on arid basin runoff: Case study: Azamharat river basin, Yazd, Iran", *4th Conferences on Water Resources Management*, Iran, Tehran (2011).
 17. Salmon, S., Qin, D., Manning, M., Chen, Z., Marquis, M., Averyt, K.B., Tignor, M. and Miller, H.L. "Summary for policymakers, the physical science basis, contribution of working group I to the fourth assessment report of the intergovernmental panel on climate change" IPCC (2007).
 18. Semenov, M.A. "A stochastic weather generator for use in climate impact studies LARS-WG user manual version 3.0", Long Ashton Research Station, UK (2003).
 19. Racsco, P., Szeidl, L. and Semenov, M. "A serial approach to local stochastic weather model", *Journal of Ecological modeling*, **57**, pp. 27-41 (1991).
 20. Nguyen, V-T-V., Nguyen, T-D. and Cung, A. "A statistical approach to downscaling of sub-daily extreme rainfall processes for climate-related impact studies in urban areas", *Water Science & Technology: Water Supply*, **7(2)**, pp. 183-192 (2007).
 21. Wilby, R.L., Dawson, C.W. and Barrow, E.M. "SDSM - A decision support tool for the assessment of regional climate change impacts", *Environmental Modeling & Software*, **17**, pp. 147-159 (2002).

Biographies

Amir Pourtouserkani was born in Shiraz, Iran, in 1973. He obtained his BS degree in Civil Engineering from Shiraz University, Shiraz, Iran, in 1995, and his MS degree in Civil Engineering from Amir Kabir University, Tehran, Iran, in 1998.

He has worked with a number of companies on projects in the field of Water Engineering. He is currently working towards his PhD degree at Shiraz University, Iran, while also working in the Petrochemical Industry and Design Engineering Company (PIDEC) as a design engineer.

He has also published numerous scientific papers in his field of interest.

Gholamreza Rakhshandehroo received his BS degree from Shiraz University, Iran, in 1985, and his MS and PhD degrees from Michigan State University, USA, in 1997. Currently, he is Professor of Civil Engineering at Shiraz University, Iran, where he undertakes teaching and research, and is also Vice Chancellor of student affairs.